

THE CEILING JET IN FIRES



Howard W. Emmons

**Harvard University
Division of Applied Sciences
Cambridge, MA**

**Sponsored by:
U.S. DEPARTMENT OF COMMERCE
National Institute of Standards
and Technology
National Engineering Laboratory
Center for Fire Research
Gaithersburg, MD 20899**

**U.S. DEPARTMENT OF COMMERCE
Robert A. Mosbacher, Secretary
NATIONAL INSTITUTE OF STANDARDS
AND TECHNOLOGY
John W. Lyons, Director**

NIST

111 111

111 111

THE CEILING JET IN FIRES

Howard W. Emmons

**Harvard University
Division of Applied Sciences
Cambridge, MA**

**October 1990
Issued December 1990**

NIST Grant No. 60NANB8D0845

**Sponsored by:
U.S. DEPARTMENT OF COMMERCE
National Institute of Standards
and Technology
National Engineering Laboratory
Center for Fire Research
Gaithersburg, MD 20899**



**U.S. DEPARTMENT OF COMMERCE
Robert A. Mosbacher, Secretary
NATIONAL INSTITUTE OF STANDARDS
AND TECHNOLOGY
John W. Lyons, Director**

Notice

This report was prepared for the Center for Fire Research of the National Institute of Standards and Technology under Grant Number 60NANB8D0845. The statements and conclusions contained in this report are those of the authors and do not necessarily reflect the views of the National Institute of Standards and Technology or the Center for Fire Research.

The CEILING JET in FIRES

Howard W. Emmons
Division of Applied Sciences
Harvard University

October 25, 1990

Home Fire Project Technical Report No. 82

INTRODUCTION

This report is a review of the state of the art of the ceiling jet phenomenon in fires. The ceiling jet is the layer of hot gases that forms above a fire, and it is the primary source of heat transfer to the ceiling and the upper part of the room. The ceiling jet is characterized by its temperature, velocity, and thickness. The temperature of the ceiling jet is typically between 1000 K and 1500 K, and its velocity is typically between 0.5 m/s and 1.0 m/s. The thickness of the ceiling jet is typically between 0.1 m and 0.2 m. The ceiling jet is formed by the buoyancy of the hot gases, and it is the primary source of heat transfer to the ceiling and the upper part of the room. The ceiling jet is characterized by its temperature, velocity, and thickness. The temperature of the ceiling jet is typically between 1000 K and 1500 K, and its velocity is typically between 0.5 m/s and 1.0 m/s. The thickness of the ceiling jet is typically between 0.1 m and 0.2 m.

The ceiling jet is the layer of hot gases that forms above a fire, and it is the primary source of heat transfer to the ceiling and the upper part of the room. The ceiling jet is characterized by its temperature, velocity, and thickness. The temperature of the ceiling jet is typically between 1000 K and 1500 K, and its velocity is typically between 0.5 m/s and 1.0 m/s. The thickness of the ceiling jet is typically between 0.1 m and 0.2 m. The ceiling jet is formed by the buoyancy of the hot gases, and it is the primary source of heat transfer to the ceiling and the upper part of the room. The ceiling jet is characterized by its temperature, velocity, and thickness. The temperature of the ceiling jet is typically between 1000 K and 1500 K, and its velocity is typically between 0.5 m/s and 1.0 m/s. The thickness of the ceiling jet is typically between 0.1 m and 0.2 m.

THE CEILING JET IN FIRES

Howard W. Emmons
Harvard University
Division of Applied Sciences
Cambridge, Massachusetts 02138

The steady ceiling jet is examined with a simplified "top hat" theory. Friction causes the jet to change downstream with flow, depth, and/or hydraulic jump adjustments to produce Richardson Number = 1 at the corridor exit, just as in hydraulics. Entrainment has a qualitative effect identical to friction, although there are quantitative differences. Heat transfer has, however, the opposite effect; the Richardson Number moves away from 1 as the flow proceeds. When all effects are included, high friction cases are predictable, while low friction cases are not. New experimental studies are needed to locate the reasons.

INTRODUCTION

As a fire grows in a room, a plume of hot, smoky gas rises to and spreads out on the ceiling. Initially, the cooling by the ceiling so decreases the buoyancy that the ceiling jet, when reaching the room walls, turns and flows downward toward the floor. After a few seconds, the general room circulation is replaced by a stable hot layer, which increases in depth and temperature until the layer interface reaches the door soffit and the hot gas flows out of a door into the next room or a corridor. A new ceiling jet is then formed and the phenomena are repeated in the corridor.

There are a number of important fire effects produced by the ceiling jet. The initial brief room circulation at the start of a fire is of little importance, although the initial depth and temperature along the ceiling are important for activation of smoke detectors or

sprinklers. The assumption made by most fire models of instantaneous spread of fire gases over the ceiling is usually adequate for small rooms. However, in a large ballroom or warehouse, the assumption of instantaneous spread is seriously wrong. Instant spread produces a uniform hot layer which heats to ignition objects far from the fire almost as fast as objects close to the fire. In fact, distant objects ignite too soon and the ignition of nearby objects is improperly delayed. In some cases, the heating, pyrolysis, burning, and/or collapse of the ceiling over the fire plume is seriously delayed by an instant spread model. Finally, the real fire may soon have flames which reach and spread out over the ceiling. These also produce a very hot ceiling immediately above the plume well before flames reach more distant points.

When the hot gases flow out of a fire room into a long corridor, they may move directly out at ceiling level or more likely rise in a plume from the door soffit to the corridor ceiling. If it is a long corridor, the time taken for the ceiling jet to reach the far end is an important time delay for the safety of building occupants at the far end. As the hot gas advances, it cools and may become too cool to remain bouyant, in view of general air currents. As a consequence, the ceiling jet falls and mixes with the lower cold layer and moves back toward the fire. The hot front then advances much more slowly. At the same time, the ceiling by the fire room door may be heated to pyrolysis, and/or eventual failure. Excess fuel gases from the fire room and/or by pyrolysis of the ceiling may burn as a flame in the ceiling jet and thus maintain the jet at high temperature and buoyancy.

When an advancing ceiling jet reaches the end of a corridor, it will simply flow out, if the corridor is completely open or, if not, it will turn downward and appear to return under the advancing layer or if the door soffit is high enough, some of the jet fluid will flow out. When a reflected jet appears to return, it actually stops the advancing stream as a hydraulic jump moves upstream.

The initial ceiling jet advance occurs at a Froude number of about 1 with a bulbous front. While many details are known⁽¹⁻⁴⁾ they are of little importance to fire safety engineering.

There are three theoretical approaches to the ceiling jet phenomena. Field modeling -- the numerical solution of the Navier-Stokes equations -- is the most complete and most accurate.^(1,2) While presumably capable of answering all questions, they are most useful for research because of the cost and time of a very large computer. Because of this, most work has been done using boundary layer theory or a model with a preassigned velocity and temperature profile.⁽⁵⁻⁸⁾ These theories, jointly with an experimental program, usually can be made to fit the data and have resulted in various useful practical formulas.

In this paper, the simplest theory, top hat velocity and temperature profile, is used to study the effects of friction, entrainment, and heat transfer and to develop useful simple formulas for fire modeling. The problem considered is also the simplest; a long, straight corridor with a smooth ceiling and open at its end.

GENERAL EQUATIONS

By reference to Figure 1, the following basic equations are obtained.

Conservation of Mass

$$\frac{dm}{dx} = E\rho u \quad (1)$$

The entrainment rate is thus assumed proportional to the local jet mass flux. The mass flux per unit width of corridor is

$$\dot{m} = \rho u \delta \quad (2)$$

Conservation of Momentum

$$\frac{d\dot{m}u}{dx} = -g'\rho\delta\frac{d\delta}{dx} + \frac{g\delta^2}{2}\frac{d\rho}{dx} - \frac{f}{2}\rho u^2 \quad (3)$$

where

$$g' = g \frac{\rho_a - \rho}{\rho} \quad (4)$$

first term. The mass flux must be inside the derivative, since the entrained air must be accelerated by the jet flow.

second term. The pressure force on the downstream face of the element is higher than on the upstream face because the depth increment, $d\delta$, has fluid ρ downstream and fluid ρ_a upstream, and the resultant pressure increment $g(\rho_a - \rho)d\delta$ acts on the whole jet depth δ .

third term. The hydrostatic pressure is higher on the upstream face than the downstream face, if the density increases with x .

fourth term. Wall friction acts against the jet motion.

Conservation of Energy

$$\frac{d\dot{m}c_p(T - T_a)}{dx} = -h(T - T_a) \quad (5)$$

Again, the mass flux appears inside the derivative because air is entrained. The derivation is most direct, if ambient temperature is assumed to be the energy datum. The heat transfer coefficient h includes convective heat transfer to the ceiling at T_a plus linearized radiative heat transfer to the ceiling and ambient temperature objects below.

THE BASIC FLOW

Consider first a hot perfect fluid ceiling jet with no friction, no entrainment, and no heat transfer. The basic equations then become

$$(1 - Ri) \frac{d\delta}{dx} = 0 \quad (6)$$

where

$$Ri = \frac{1}{Fr^2} = \frac{g' \delta}{u^2} = \frac{g' \delta^3}{Q^2} = \frac{g' Q}{u^3} \quad \text{Richardson Number} \quad (7)$$

$$Q = u \delta = \frac{\dot{m}}{\rho} \quad \text{volume flow per unit width} \quad (8)$$

Equation (6) indicates that the jet depth cannot change ($d\delta = 0$) unless the Richardson Number equals 1. As is well known, the wave speed on the interface of a shallow, buoyant layer ($d\delta \neq 0$) is equal to $\sqrt{g' \delta}$ and $Ri = Fr = 1$. Thus, the fluid is moving at the wave speed $u = \sqrt{g' \delta}$ and any variation of the depth would remain stationary.

If $Ri < 1$ ($Fr > 1$) shooting flow, the fluid velocity is greater than the wave speed. Thus, any disturbance ($d\delta \neq 0$) would be carried out the end of the corridor. Similarly, if $Ri > 1$ ($Fr < 1$) tranquil flow, the fluid velocity is less than that of a surface wave which, therefore, moves upstream to the source of the fluid.

THE EFFECT OF CEILING FRICTION

With no heat transfer nor entrainment, the density, ρ , and volume flow per unit width, Q , are constant. Equations (3) and (4) then yield

$$(1 - Ri) \frac{d\delta}{dx} = \frac{f}{2} \quad (9)$$

Thus, if

$$Ri \begin{cases} > 1 \\ = 1 \\ < 1 \end{cases} \quad \text{then} \quad \frac{d\delta}{dx} \begin{cases} < 0 & \text{tranquil flow} \\ = \infty & \text{critical flow} \\ > 0 & \text{shooting flow} \end{cases} \quad (10)$$

a tranquil flow is deeper than and decreases to critical while a shooting flow is less deep than and increases to critical. By equation (7), the critical flow depth is given by

$$\delta_c^3 = \frac{Q^2}{g'} \quad (11)$$

and using this

$$Ri = \left(\frac{\delta}{\delta_c} \right)^3 \quad (12)$$

Equation (9) with the origin at $\frac{\delta}{\delta_c} = 1$ integrates to

$$\frac{\delta}{\delta_c} - \frac{1}{4} \left(\frac{\delta}{\delta_c} \right)^4 - \frac{3}{4} = \frac{f}{2} \frac{x}{\delta_c} \quad (13)$$

The resultant depth, Figure 2, varies as in equation (10).

If the corridor is open and ends before the critical flow is reached, the ceiling jet flows out. However, since it is buoyant, the free outflowing jet rises, increases in velocity and decreases in depth. If the flow is tranquil, the decreased depth moves as a wave upstream to the source to produce a lower Richardson number (higher velocity, smaller depth) ceiling jet. This process will continue until critical flow exists at the corridor exit after which no more depth changes can enter. If the flow is shooting, $Ri < 1$, the jet will merely shoot out of the corridor unchanged. No waves can flow upstream.

If critical flow is reached before the end of the corridor, the flow cannot proceed further. The available momentum is needed for the rapid depth increase, none is available to counter additional friction force. If the flow is tranquil, pressure waves again move upstream, increasing the depth, decreasing the velocity, increasing the magnitude of $(1 - Ri)$, and by equation (10), decreasing $d\delta / dx$. Thus, the slower flow has less friction force and goes further before a critical condition is reached. This process continues until, again, critical flow is established at the exit. If the flow is shooting, waves cannot move upstream, yet the flow cannot proceed. The fluid piles up producing a finite jump in depth to a tranquil flow with a lower velocity and decreased friction. Thus, a hydraulic jump is produced which changes the shooting flow into a tranquil flow, which can proceed further. The hydraulic jump (a discontinuity in the present simple theory, but actually requiring a length of one or more jet depths) moves upstream until the tranquil flow reaches critical at the end of the corridor.

To compute a specific case, use must be made of the well known hydraulic jump formula⁽⁹⁾.

$$\frac{\delta_2}{\delta_1} = \frac{1}{2} \left((1 + 8 Fr^2)^{1/2} - 1 \right) \quad (14)$$

Since δ_c is not changed by the jump, trial jumps can be put in several places along the corridor and, for each case, the location of the critical flow of the resultant tranquil flow can be computed from Figure 2 (or equation (13)). The correct position is that which puts the critical flow at the open end.

The discussion, so far, is identical to the corresponding effects in hydraulic channel flows.⁽¹⁰⁾

THE EFFECT OF ENTRAINMENT

The direct effect of entrainment is to add mass to the ceiling jet flow according to equation (1). However, it also changes the jet temperature and density according to the energy equation (5). With the heat transfer coefficient $h = 0$, equation (5) becomes

$$\frac{d m (T - T_a)}{dx} = 0 \quad (15)$$

with solution

$$\frac{T - T_a}{T_0 - T_a} = \frac{\dot{m}_0}{\dot{m}} \quad (16)$$

Thus, the momentum equation not only contains the variable mass flow, but g' and ρ are variable and the density derivative must be retained. Thus, the entrainment places a drag on the ceiling jet because of the need to accelerate the added mass and the density variation makes the momentum equation as complex as the completely general case.

In this section, the drag effect is examined by assuming the temperature and density are constant. The general case is examined in a later section.

$$\frac{dQ}{dx} = E u \quad (17)$$

and

$$\frac{d \delta u^2}{dx} = -g' \delta \frac{d\delta}{dx} \quad (18)$$

Eliminating dQ / dx results in

$$(1 - Ri) \frac{d\delta}{dx} = 2 E \quad (19)$$

Thus, the acceleration of the entrained fluid puts a drag on the ceiling jet and the flow behaves the same as with friction; namely, shooting flow depth increases to critical, while tranquil flow depth decreases to critical.

In this case, it is not possible to solve equation (19) directly since both Q and δ are variable. However, by integrating (18) and eliminating u and $Q (= u \delta)$ from (17) an integrable equation results in

$$\frac{3}{2} \left(\frac{\delta}{\delta_c} - 3^{-1/2} \ln \frac{3^{1/2} + \frac{\delta}{\delta_c}}{3^{1/2} - \frac{\delta}{\delta_c}} \right) - .3595 = \frac{E x}{\delta_c} \quad (20)$$

where, again, $x = 0$ at the critical flow location. The critical flow depth in terms of the initial depth δ_0 and the Froude number is obtained by integrating equation (18) and eliminating u by Fr to get

$$\left(\frac{u_0}{u_c}\right)^2 \frac{1}{2} \left(3 \frac{\delta_c}{\delta_0} - \frac{\delta_0}{\delta_c} \right) = \frac{\delta_0}{\delta_c} Fr_0^2 \quad (21)$$

from which follows

$$\frac{\delta_c}{\delta_0} = \left\{ \frac{1}{3} (2 Fr_0^2 - 1) \right\}^{1/2} \quad (22)$$

It may appear odd that equation (22) does not contain the entrainment constant E . Actually, E controls the distance of the source from critical through equation (20). Equation (20) is shown in Figure 2. Equation (21) is required because the variability of Q precludes the use of equation (11) in finding δ_c . Figure 3 shows that entrainment has qualitatively the same effect on the flow as friction, but with quantitative differences.

THE EFFECT OF HEAT TRANSFER

With entrainment and friction neglected, the momentum equation (3) reduces to

$$u \frac{du}{dx} = -g' \frac{d\delta}{dx} + \frac{g\delta}{2\rho} \frac{d\rho}{dx} \quad (23)$$

This, together with the constant mass flow equation (2) gives

$$(1 - Ri) \frac{d\delta}{dx} = \delta \left(1 + \frac{T_a}{2(T - T_a)} Ri \right) \frac{1}{T} \frac{dT}{dx} \quad (24)$$

where $\rho T = \text{constant}$ was used to replace ρ by T .

We note that for a fire ceiling jet, which cools as it flows along, the temperature drops and the right side of equation (24) is negative. It follows that

$$\text{For } Ri \begin{cases} > 1 \\ = 1 \\ < 1 \end{cases} \quad \text{then } \frac{d\delta}{dx} \begin{cases} > 0 & \text{tranquil flow} \\ = \infty & \text{critical flow} \\ < 0 & \text{shooting flow} \end{cases} \quad (25)$$

By comparing this with the previous cases, equation (10), we see that the effect on the ceiling jet growth is opposite; namely, tranquil flow increases in depth while shooting flow becomes less deep.

Since Ri is dependent upon both T and δ , equation (24) cannot be integrated analytically. Using equations (7) and (4) in the form

$$d \ln Ri = d \ln g' + 3 d \ln \delta + 2 d \ln \rho \quad (26)$$

$$d \ln g' = \left(\frac{T_a}{T - T_a} + 2 \right) d \ln T \quad (27)$$

and eliminating $d \ln \delta$ between equations (24) and (26) results in

$$\frac{(1 - Ri)}{Ri(2 + Ri)} \frac{d Ri}{dT} = \frac{1}{2} \frac{2T - T_a}{T(T - T_a)} \quad (28)$$

With the boundary condition at $x = 0$; $Ri = Ri_0$ and $T = T_0$, this integrates to

$$\frac{Ri}{(2 + Ri)^3} = \frac{Ri_0}{(2 + Ri_0)^3} \frac{T - T_a}{T_0 - T_a} \frac{T}{T_0} \quad (29)$$

The relation between $0 < Ri < \infty$ and $Ri / (2 + Ri)^3$ is shown in Figure 3. The critical condition at $Ri = 1$ appears as the maximum in this function. Since the temperature terms on the right start at 1 and decrease to zero as the ceiling jet cools, the flow Richardson Number solution runs down the curve in Figure 3, as shown by the arrows -- tranquil flow to the right, shooting flow to the left.

The density terms can be found in terms of the distance along the corridor by integration of equation 5.

$$T - T_a = (T_0 - T_a) e^{-\zeta} \quad (30)$$

where

$$\zeta = \frac{h x}{\dot{m} c_p} \quad (31)$$

Thus, the $Ri(\zeta)$ relation becomes

$$\frac{Ri}{(2 + Ri)^3} = \frac{Ri_0}{(2 + Ri_0)^3} \left\{ \frac{T_a}{T_0} + \left(1 - \frac{T_a}{T_0} \right) e^{-\zeta} \right\} e^{-\zeta} = \frac{Ri_0}{(2 + Ri_0)^3} \frac{T}{T_0} e^{-\zeta} \quad (32)$$

For the effect of friction, equation (13), or entrainment, equation (20), all parameters and boundary conditions are absorbed into the variables so general curves, Figures 2 and 3, could be presented independent of any specific case.

For equation (32), the initial-to-ambient temperature and the initial Richardson Number Ri_0 remain as parameters. To show the nature of the solution of equation (32), the case of Column I of Table 1 is used. Figures 4 and 5 show that for tranquil flow both Richardson Number and the layer depth increase indefinitely while, for shooting flow, the Richardson Number goes to zero (because $\rho \rightarrow \rho_a$) while the ceiling jet depth and velocity become asymptotic to finite values.

To appreciate how rapid these heat transfer effects really are, the physical distance along the corridor is

$$x = \frac{\dot{m} c_p}{h} \zeta = 4.050 \zeta \quad (33)$$

Thus, $\zeta = 5$ corresponds to x of only 20.25 meters. Many corridors are longer than this and yet even at this distance, the Richardson Number for tranquil flow is of the order of 100 and the ceiling jet depth is 12.9 times its initial depth. At this point, the effective gravity, $g' = .110$, is only about one percent of g . The ceiling jet has so little buoyancy left that it cannot remain at the ceiling against the usual room currents. The ceiling jet will fall, mix with the return air in the lower layer, thus being carried back into the fire. The above computation was made with equation (32) using

$$y^3 = \left(\frac{\delta}{\delta_0} \right)^3 = \frac{Ri}{Ri_0} \left(\frac{T}{T_0} \right)^2 e^\zeta \quad (34)$$

to compute the ceiling jet depth.

If the depth is to be computed directly, Ri can be eliminated between equation (32) and (34) to get the cubic equation for y

$$Ri_0 \left(\frac{T_0}{T} \right)^2 e^{-\zeta} y^3 - (2 + Ri_0) \frac{T_0}{T} y + 2 = 0 \quad (35)$$

We note that the requirement for tranquil flow, that $Ri = 1$ at the end of an open corridor cannot be met by any of the available solutions. We return to this question in the concluding section.

GENERAL CEILING JET WITH FRICTION, ENTRAINMENT, AND HEAT TRANSFER

The general equations have not been analytically solved, but following the general methods used in the last section, the results can be put into several useful forms.

$$\frac{1 - Ri}{Ri(2 + Ri)} \frac{d Ri}{d \zeta} = \frac{1}{2} \frac{2T - T_a}{(T - T_a)T} \frac{dT}{d \zeta} + \frac{3 f}{2 H y(2 + Ri)} + \frac{2 E}{H y} \quad (36)$$

where

$$y = \frac{\delta}{\delta_0}$$

Again, the first two terms can be integrated, while the last two remain to be numerically evaluated.

$$\frac{Ri}{(2 + Ri)^3} = \frac{Ri_0}{(2 + Ri_0)^3} \frac{T - T_a}{T_0 - T_a} \frac{T}{T_0} e^{3 \frac{f}{H} \int_0^\zeta \frac{d \zeta}{y(2 + Ri)}} e^{4 \frac{E}{H} \int_0^\zeta \frac{d \zeta}{y}} \quad (37)$$

Because of entrainment, the mass flux is not constant, but is given by

$$\frac{\dot{m}}{\dot{m}_0} = e^{\frac{E}{H} \int_0^{\zeta} \frac{d\zeta}{y}} \quad (38)$$

The energy equation must be integrated with due regard to the mass flow change. Thus,

$$\frac{T - T_a}{T_0 - T_a} = \frac{\dot{m}_0}{\dot{m}} e^{-\int_0^{\zeta} \frac{\dot{m}_0}{\dot{m}} d\zeta} \quad (39)$$

which reduces to equation (3), if there is no entrainment. Finally, the temperature terms can be replaced by functions of position. Thus,

$$\frac{Ri}{(2 + Ri)^3} = \frac{Ri_0}{(2 + Ri_0)^3} \left\{ \frac{T_a}{T_0} + \left(1 - \frac{T_a}{T_0} \right) \frac{\dot{m}_0}{\dot{m}} e^{-\int_0^{\zeta} \frac{\dot{m}_0}{\dot{m}} d\zeta} \right\} \left(\frac{\dot{m}}{\dot{m}_0} \right)^3$$

$$e^{-\int_0^{\zeta} \frac{\dot{m}_0}{\dot{m}} d\zeta} e^{3 \frac{f}{H} \int_0^{\zeta} \frac{d\zeta}{y(2 + Ri)}} \quad (40)$$

This set of equations contains four parameters, $\frac{T_a}{T_0}$, Ri_0 , $\frac{E}{H}$, $\frac{f}{H}$,

and has not yet been fully explored. However, it is clear from equation (34) that the friction and entrainment counteract the effect of the heat transfer. In fact, f and E are most effective in mid-range after the very large temperature gradient is past and before the large depth and low velocity make them ineffective.

THE EFFECT OF FRICTION AND HEAT TRANSFER

We look at the ceiling jet flow without entrainment. Because of the buoyancy, turbulence and entrainment are somewhat suppressed. Atallah⁽¹¹⁾ found values of $E = .003$ when burning was present. See also Ellison and Turner.⁽¹²⁾ In this case, the mass flow is constant and equation (38) reduces to

$$\frac{Ri}{(2 + Ri)^3} = \frac{Ri_0}{(2 + Ri_0)^3} \left\{ \frac{T_a}{T_0} + \left(1 - \frac{T_a}{T_0} \right) e^{-\zeta} \right\} e^{-\zeta} e^{3 \frac{f}{H} \int_0^\zeta \frac{d\zeta}{y(2 + Ri)}} \quad (41)$$

This equation has been solved numerically by evaluating the integral step by step and at each step solving the entire equation for Ri by a bisection root-finding algorithm. There are many alternative procedures possible, but this seemed best for avoiding difficulties at $Ri = 1$.

The solutions for the case of Column 1, Table 1, are shown in Figures 6 and 7 for an initial $Ri_0 = 1$. For shooting flow, all solutions start with negative infinite slope, while for tranquil flow, almost all solutions start with positive infinite slope. One limit case with $f = .0826375$ appears to start at a finite slope. The reason for the large number of decimals (the limit of my single precision) is that a change by 1 in the last place has no solutions starting at $Ri = 1$. We return to this point later in this section.

By setting $Ri_0 = 2$, the solutions look as in Figures 8 and 9. Ignoring the line to point 0, all solutions either loop down to $Ri = 1$ for large f , or swoop up to infinity for small f . Again, a change of 1 in the last place makes the flip. (This could have been followed to many more decimal places, if desired.)

To understand this behavior, the differential equation (36) is put into the form
 ($dT / d\zeta$ eliminated with the energy equation (5), $E = 0$, m constant)

$$\frac{d Ri}{d\zeta} = \frac{Ri}{2y} \left\{ \frac{\frac{3f}{H} - (2 + Ri) \left(2 - \frac{T_a}{T}\right) y}{1 - Ri} \right\} \quad (42)$$

Then, eliminating y from the numerator, using equation (34), we get

$$\frac{d Ri}{d\zeta} = \frac{Ri}{2y} \left(\left(\frac{T}{T_0} \right)^2 e^{-\zeta} \right)^{1/3} \left(2 - \frac{T_a}{T} \right) \frac{f}{H} \left\{ \frac{3 \left(\left(\frac{T_0}{T} \right)^2 e^{-\zeta} \right)^{1/3} \left(1 - \frac{T_a}{T} \right)^{-1} - \frac{H Ri^{1/3} (2 + Ri)}{f Ri_0^{1/3}}}{1 - Ri} \right\} \quad (43)$$

From this we see that

$$\frac{d Ri}{d\zeta} = \infty \quad \text{at} \quad Ri = 1 \quad (44)$$

$$\frac{d Ri}{d\zeta} = 0 \quad \text{at} \quad r = \varphi(\zeta) \quad (45)$$

$$r = \frac{H Ri^{1/3} (2 + Ri)}{f Ri_0^{1/3}} \quad (46)$$

where

$$\varphi(\zeta) = 3 \left(\left(\frac{T_0}{T} \right)^2 e^{-\zeta} \right)^{1/3} \left(2 - \frac{T_a}{T} \right)^{-1} \quad (47)$$

$$\frac{T}{T_a} = 1 + \left(\frac{T_0}{T_a} - 1 \right) e^{-\zeta} \quad (48)$$

Figure 10 shows the solutions to Figures 8 and 9 plotted as r vs ζ with the additional line, equation (47), dependent only upon the ambient and initial temperatures and the heat transfer coefficient. All solutions do indeed cross this line horizontally and divide between those that increase to infinity and those that fall to $Ri = 1$.

The point 0 at $\zeta = 4.683$, Figure 10, where both numerator and denominator are zero is a node. Since the coefficient in equation (43) is always positive, while the numerator and denominator are negative above and positive below their respective lines, the solution curves have slopes indicated by the $+$ and $-$ signs around the node, which is a saddle point.

At point 0, the solution slope must be evaluated as a $0/0$ form, see Appendix A for details. The resultant solution slopes at the node are

$$\left. \frac{d Ri}{d \zeta} \right|_n = 1 - \left(1 \pm \sqrt{3} \right) \frac{T_a}{2 T_n} \quad (49)$$

where T_n is the jet temperature at the node. The corresponding slopes in Figure 10,

shown  are given by

$$\left. \frac{dr}{d\zeta} \right|^n = \frac{2}{3} r_n \left\{ 1 - \left(1 \pm \sqrt{3} \right) \frac{T_a}{2 T_n} \right\} \quad (50)$$

Although the solution curve from $\zeta = 0$ to $\zeta = \zeta_n$ cannot conveniently be obtained by integration from $\zeta = 0$ because the equation becomes very stiff as $\zeta \rightarrow \zeta_n$, it is easy to begin at $\zeta = \zeta_n$ and integrate toward $\zeta = 0$. The solution is started at the node with an initial slope given by equation (49) and then continued by integration backward, using equation (41) in the form

$$\frac{Ri}{(2 + Ri)^3} = \frac{\left(1 + \left(\frac{T_0}{T_a} - 1 \right) e^{-\zeta} \right) e^{-\zeta}}{27 \left(1 + \left(\frac{T_0}{T_a} - 1 \right) e^{-\zeta_n} \right) e^{-\zeta_n}} e^{\frac{3f}{H} \int_{\zeta_n}^{\zeta} \frac{d\zeta}{y(2 + Ri)}} \quad (51)$$

The integration requires a value of the friction factor and y_n . Since the various solution curves in Figure 10 approach each other as we move to smaller ζ , the value of f is not critical. $f = .12920$ was used. The nodal ceiling jet depth is computed by

$$y_n^3 = \frac{1}{Ri_0} \left(\frac{T_c}{T_0} \right)^2 e^{\zeta_n} \quad (52)$$

The results are the lines from NODE in Figures 8 through 10.

We now return to Figure 6 and note that the starting point is a node, if $Ri_0 = 1$, and $r = \varphi(0)$, equation (45), and the numerator of equation (43) = 0 (satisfied by $f = .08264375$ in this case). The two slopes given by equation (49) are shown



Thus, the starting point is a saddle point node.

The shooting flows, which rise and cross $Ri = 1$ at a finite ζ , as the curve $f = .07$ at $\zeta = .96$ in Figure 6, does so at a node passing straight through from shooting to tranquil flow without a hydraulic jump.

THE CEILING JET

In this section, we apply the above theory to an arbitrary fire-produced ceiling jet in tranquil flow in an open-ended corridor of arbitrary length. Such a case is defined by the parameters \dot{m} , T_0 , T_a , h , f , L , Ri_0 . We note immediately that Ri_0 may be altered by the $Ri = 1$ control at the open end.

To solve this problem, we first calculate ζ at the end.

$$\zeta_e = \frac{h L}{\dot{m} c_p} \quad (53)$$

From this, we find the sign of the numerator in brackets of equation (42) in the form

$$N = \frac{f}{h / \dot{m} c_p} - \left(2 - \frac{T_a}{T_e} \right) \delta_e \quad (54)$$

where $Ri = 1$, and δ_0 has been canceled out.

$$\delta_e = \left(\frac{\dot{m}^2}{\rho_e^2 g_e} \right)^{1/3} \quad (55)$$

For $Ri > 1$ in the corridor, $d Ri / d \zeta$ is opposite in sign to N .

If $N > 0$, the corridor ends before the node is reached. The solution to equation (51) will start at $Ri = 1$ and $\zeta = \zeta_e$ with minus infinite slope and curve back to Ri_0 at $\zeta = 0$. Thus, the ceiling jet depth and velocity at the source will be altered appropriately.[§]

If $N = 0$, the corridor end is at the node and the backward solution to equation (51), beginning at $\zeta_0 = \zeta_e$, must start with the negative slope given by equation (50). Again, Ri_0 will come from the solution and requires source adjustment.[§]

If $N < 0$, the corridor ends after the node and the solution slope for $Ri > 1$ is positive. The solution starting at the end does so with positive infinite slope and moves toward $\zeta > \zeta_e$. No solution starting with $Ri = 1$ at the end exists for $\zeta < \zeta_e$. See the concluding section for further comments on this case.

COMPARISON WITH EXPERIMENT

Although there are many papers on ceiling jet measurements,⁽¹³⁻¹⁵⁾ few are detailed enough to guide the theory. A recent Ph.D. thesis by M. V. Chobotov⁽¹⁶⁾ provides both careful measurements over a narrow range of conditions and a careful boundary layer theory with appropriate velocity and temperature profiles. This theory failed completely to fit the data and was abandoned in favor of the completely unfounded assumption that $Ri = 1$ everywhere. This assumption agreed fairly well with the data (see Figures 11 and 12).

The top-hat theory developed here was applied to the Chobotov experiment computed with the data of Column II, Table 1. The results are shown in Figures 11, 12, and 13. This computation from $\zeta = 0$ contains a node far short of the end of the experimental channel and shows why Chobotov's boundary layer theory solution failed.

[§] "Source adjustment" does not mean any effect on the fire. It means a change of velocity and depth after the fire plume reaches the ceiling.

The solution with $f = .0359008$ (7 decimal places) reaches the end

$$\zeta_e = \frac{h L}{\dot{m} c_p} = 2.0986 \quad \text{at } Ri \text{ about } 3 \text{ and } y_e = 2.5 \text{ much larger than the experimental}$$

values. (The experiment does not reach $Ri = 1$ at the end perhaps because the measurements ceased one meter from the end.)

An attempt to correct the theoretical prediction was made by moving the node to the end. To do this, we set $r_e = 1.67928$ by equation (45). At the source, the solution must

$$\text{be close to } r_0 = \varphi(0) = 2.4292. \quad \text{By definition } Ri_0 = \frac{g'_0 \rho_0^2 \delta_0^3}{\dot{m}_2} = 4062.9 \delta_0^3.$$

Also, the heat transfer factor

$$H = \frac{h \delta_0}{\dot{m} c_p} = .41897 \delta_0 \quad (56)$$

Thus

$$r_0 = 2.4292 = \frac{H (2 + Ri_0)}{f} = \frac{.83794 \delta_0 + 1702.2 \delta_0^4}{f} \quad (57)$$

However,

$$r_e = 1.67928 = \frac{3 H}{f Ri_0^{1/3}} = \frac{3.41897 \delta_0}{f (4062.9)^{1/3} \delta_0} = \frac{.078770}{f} \quad (58)$$

$$\text{Thus, } f = .046907^*$$

* This value of f required to move the node to the end seems rather large in view of the fact that the experiment suggested the friction to be negligible.

and $\delta_0 = .074248$ as the root of

$$1702.2 \delta_0^4 + .83794 \delta_0 - .113947 = 0 \quad (59)$$

Finally, the expected $Ri_0 = 1.66302$. The solution was obtained by backward integration (the solution should be iterated, if Ri_0 differs too much from the above approximate value). In this case, the value was $Ri_0 = 1.6084$, which was taken as satisfactory.

This calculation, shown on Figures 11, 12, and 13, was poor for layer depth and way off for Ri . The unfounded assumption $Ri = Ri_0$ following Chobotov's $Ri = 1$ assumption agrees somewhat better.

CONCLUSIONS

The simple top-hat type theory used in this paper would be expected to yield a correct qualitative semi-quantitative solution to the flow of buoyant fire gases along a ceiling. So long as the corridor is not too long, the heat transfer not too large, or the friction and entrainment not too small, reasonable-looking results are obtained satisfying the open end outlet condition for tranquil flow of Richardson Number = Froude Number = 1.

However, for many cases, there appears to be no solution satisfying $Ri = 1$ at the end. The reason for this is not clear. If the ceiling jet arrives at the open end with $Ri > 1$, the jet is too deep and the fluid "falls out" with acceleration. Thus, the adjustment could take place beyond the end of the corridor.

If this were the case, the increased velocity and decreased depth would be expected to propagate upstream at the wave speed $\sqrt{g' \delta}$ which is higher than the end fluid

velocity. Since it is the wave speed which suggests that upstream effects are expected, but that the thermal effects prevent such adjustments, we might suppose that the thermal effects change the wave speed. A new shallow water wave analysis has not yet been successful, but this does not seem to be the solution to this problem. The correct explanation would appear to be either non top-hat adjustments at and just outside of the end of the corridor, or some non-steady effects with localized fluid accumulation and discharge, suggested by observations of persons fleeing from a fire who state that "the fire came rolling along the ceiling."

Another phenomena sometimes intervenes to alter the $Ri = 1$ problem. As the ceiling jet moves along the corridor and cools off, its buoyancy falls and it is more easily removed from the ceiling by drafts or other disturbances. In the case of fire, there is often a lower layer current of atmospheric air returning into the fire source. This lower level return current can entrain the extra deep, extra cool ceiling jet which, therefore, never reaches the corridor end.

It is clear that some scientifically motivated ceiling jet studies are essential to guide further theoretical work on the ceiling jet.

The theory of this paper is about the right complexity for use in a general fire model, with some empirical coefficients, if necessary. It needs to be further developed to include partially open or closed corridors. It needs to be extended to the two dimensional ceiling of a room and needs to include residual fuel which is burning. All of the above include sufficient transient effects to properly predict the growth and decay of the fire.

APPENDIX

Derivation of Node Solution Slopes

At a node, the solution slope equation (42)

$$\frac{d Ri}{d \zeta} = \frac{Ri}{2y} \left\{ \frac{\frac{3f}{H} - (2 + Ri) \left(2 - \frac{T_a}{T} \right) y}{1 - Ri} \right\} \quad (A-1)$$

takes the form

$$\left. \frac{d Ri}{d \zeta} \right|_n = \frac{1}{2 y_n} \int_{\substack{Ri \rightarrow 1 \\ \zeta \rightarrow \zeta_n}} \frac{\frac{3f}{H} - (2 + Ri) \left(2 - \frac{T_a}{T} \right) y}{1 - Ri} = \frac{1}{2 y_n} \int_n \frac{\psi(Ri, \zeta)}{1 - Ri} \Rightarrow \frac{0}{0} \quad (A-2)$$

To find the solution slopes at the node, we have to evaluate this 0/0 form by observing that, near the node, the solution slope S must point directly to the node. We thus must compute the solution slopes at $Ri = 1 + \varepsilon$, $\zeta = \zeta_n + \mu$ and set

$$S = \frac{\varepsilon}{\mu} \quad (A-3)$$

The solution slope near the node is found by Taylor series expansion about the node

$$\left. \frac{d Ri}{d \zeta} \right|_n = \frac{1}{2 y_n} \frac{\psi(1, \zeta_n) + \left. \frac{\partial \psi}{\partial Ri} \right|_n \epsilon + \left. \frac{\partial \psi}{\partial \zeta} \right|_n \mu}{-\epsilon} = -\frac{1}{2 y_n} \left(\left. \frac{\partial \psi}{\partial Ri} \right|_n + \left. \frac{\partial \psi}{\partial \zeta} \right|_n \frac{1}{S} \right)$$

(A-4)

The evaluation of these derivatives is most simply done with extensive use of the log function.

$$\left. \frac{\partial \psi}{\partial Ri} \right|_n = - \left(2 - \frac{T_a}{T_n} \right) y_n \left(1 + 3 \left. \frac{\partial \ln y}{\partial Ri} \right|_n \right) \quad (A-5)$$

$$\left. \frac{\partial \psi}{\partial \zeta} \right|_n = -3 y_n \left\{ \left(2 - \frac{T_a}{T_n} \right) \left. \frac{d \ln y}{d \zeta} \right|_n - \left. \frac{d \left(\frac{T_a}{T} \right)}{d \zeta} \right|_n \right\} \quad (A-6)$$

Using

$$3 \ln y = \ln Ri - \ln Ri_0 + 2 \ln \left(\frac{T}{T_0} \right) + \zeta \quad (A-7)$$

$$\left. \frac{d \ln y}{d Ri} \right|_n = \frac{1}{3} \quad (A-8)$$

$$\left. \frac{d \ln y}{d \zeta} \right|_n = -\frac{1}{3} \left(1 - 2 \frac{T_a}{T_n} \right) \quad (A-9)$$

where

$$\left. \frac{d \left(\frac{T}{T_0} \right)}{d \zeta} \right|_n = \frac{T_a}{T_0} - \frac{T_n}{T_0} \quad (\text{A-10})$$

has been used. Also needed is

$$\left. \frac{d \left(\frac{T_a}{T} \right)}{d \zeta} \right|_n = \frac{T_a}{T_n} \left(1 - \frac{T_a}{T_n} \right) \quad (\text{A-11})$$

Inserting all these relations into (A-5) and (A-6), we get, after some algebra

$$\left. \frac{d \psi}{d Ri} \right|_n = -2 \left(2 - \frac{T_a}{T_n} \right) y_n \quad (\text{A-12})$$

$$\left. \frac{d \psi}{d \zeta} \right|_n = y_n \left\{ 2 - 2 \frac{T_a}{T_n} - \left(\frac{T_a}{T_n} \right)^2 \right\} \quad (\text{A-13})$$

And, finally

$$\left. \frac{d Ri}{d \zeta} \right|_n = S = 2 - \frac{T_a}{T_n} - \left\{ 1 - \frac{T_a}{T_c} - \frac{1}{2} \left(\frac{T_a}{T_c} \right)^2 \right\} \frac{1}{S} \quad (\text{A-14})$$

The solution of this quadratic equation for S gives the nodal solution slopes as

$$S = 1 - (1 \pm \sqrt{3}) \frac{T_a}{2 T_n} \quad (\text{A-15})$$

Now using

$$\ln r = \ln \frac{H}{f} + \frac{1}{3} \ln Ri - \frac{1}{3} \ln Ri_0 + \ln (2 + Ri) \quad (A-16)$$

$$\left. \frac{dr}{d\zeta} \right|_n = \frac{2}{3} r_n \quad \left. \frac{d Ri}{d \zeta} \right|_n = \frac{2}{3} r_n \left(1 - \left(1 \pm \sqrt{3} \right) \frac{T_a}{2 T_n} \right) \quad (A-17)$$

NOMENCLATURE

c_p	specific heat of ceiling jet gas at constant pressure
E	entrainment coefficient, Equation (1)
f	friction factor, Equation (3)
$Fr = \frac{u}{\sqrt{g' \delta}}$	Froude Number, Equation (7)
g	acceleration of gravity
$g' = g \frac{\rho_a - \rho}{\rho}$	effective acceleration of gravity, Equation (3)
h	heat transfer coefficient, Equation (5)
$H = \frac{h \delta_0}{\dot{m} c_p}$	heat transfer factor, Equation (36)
\dot{m}	ceiling jet mass flow per unit width, Equation (2)
N	numerator of $\left. \frac{d Ri}{d \zeta} \right ^n$, Equation (54)
Q	ceiling jet volume flow per unit width, Equation (8)
$r = \frac{H (Ri)^{1/3} (2 + Ri)}{f (Ri_0)}$	useful analysis variable, Equation (43)
$Ri = \frac{g' \delta}{u^2}$	Richardson Number, Equation (7)
Ri_0	Richardson Number at jet source, Equation (29)

T	temperature
u	ceiling jet velocity
x	distance along corridor [m]
$y = \delta / \delta_0$	ceiling jet depth
δ	ceiling jet depth [m]
δ_1, δ_2	ceiling jet depth before and after a hydraulic jump, Equation (14)
$\varphi(\zeta)$	curve on which $\frac{dr}{d\zeta} = 0$, Equation (47)
$\psi(Ri, \zeta)$	numerator of $\left. \frac{d Ri}{d \zeta} \right _n$, Equation (A-2)
ρ	ceiling jet density
$\zeta = \frac{h x}{\dot{m} c_p}$	coordinate along corridor
Subscripts	
a	ambient
c	critical ($Ri = 1$)
e	open end of corridor
n	node
0	source of ceiling jet

REFERENCES

1. Baum, H. R., Rehm, R.G., and Malholland, G.W., Prediction of Heat and Smoke Movement in Enclosure Fires, *Fire Safety Journal* 6(3), 193-201, 1983.
2. Markatos, N. C., Malin, M. R., and Cox, G., Mathematical Modeling of Buoyancy Induced Smoke Flow in Enclosures, *Int. J. Heat Mass Transfer* 25, 63, 1982.
3. Benjamin, T. B., Gravity Currents and Related Phenomena, *J. Fluid Mech.* 31, 209-248, 1967.
4. Simpson, J. E. and Britter, R. E., The Dynamics of the Head of a Gravity Current Advancing Over a Horizontal Surface, *J. Fluid Mechanics* 94(3), 477-495, 1979.
5. Alpert, R., Turbulent Ceiling Jet Induced by Large Scale Fires, *Comb. Sci. and Tech.* 11, 197-213, 1975.
6. You, H. Z. and Foeth, G. M., Ceiling Heat Transfer During Plume Impingement, *Fire and Materials* 3(3), 140-147, 1979.
7. Zakoski, E.E. and Kubota, T., Experimental Study of Environment and Heat Transfer in a Room Fire, NIST-GCR-88-554 , 1988.
8. Cooper, L.Y. and Stroop, D.W., Thermal Response of Unconfined Ceilings Above Growing Fires and the Importance of Convective Heat Transfer, *Transactions of ASME* 109, 172-178, 1987.
9. Rouse, H., *Fluid Mechanics for Hydraulic Engineers*, McGraw Hill, p. 388, equation (268), 1938.
10. Channel Flow Section of any Hydraulics Text; e.g., Rouse H., *Fluid Mechanics for Hydraulic Engineers*, McGraw Hill, 273-326, 1938.

11. Atallah, S., Fires in a Model Corridor with a Simulated Combustible Ceiling, Part 1, Fire Research Station, Fire Research Notes, 620, 1966.
12. Ellison, T. H. and Turner, J. S., Turbulent Entrainment in Stratified Flows.
13. Heskestad, G. and Hill, J. P., Experimental Fires in Multiroom/Corridor Enclosures, NBS-GCR-86-502, 1986.
14. Satoh, K. and Miyazaki, S., A Numerical Study of Large Fires in Tunnels, Rys Fire Res. Inst. of Japan **68**, 19-34, 1989.
15. Sako, S. and Hasemi, Y., Response Time of Automatic Sprinklers Below a Confined Ceiling, Second Int. Symp. Fire Safety Sci., 613-622, 1989.
16. Chobotov, M. V., Gravity Currents with Heat Transfer Effects, Ph.D. Thesis, California Institute of Technology, 1987.

FIGURE CAPTIONS

- Figure 1. "Top Hat" velocity and temperature profile ceiling jet in an open-ended corridor.
- Figure 2. Effect of friction and entrainment on a ceiling jet flow
- _____ friction -- top scale
 - - - - - entrainment -- bottom scale
- Figure 3. The function $\frac{Ri}{(2 + Ri)^3}$
- Figure 4. Effect of heat transfer and initial Richardson Number on a ceiling jet Richardson Number (Case column 1, Table 1).
- Figure 5. Effect of heat transfer and initial Richardson Number on a ceiling jet depth (Case column 1, Table 1)
- Figure 6. Effect of heat transfer and friction on the Richardson Number of a ceiling jet. Initial Richardson Number = 1 (Case column 1, Table 1)

Figure 7. Effect of heat transfer and friction on a ceiling jet depth. Initial Richardson Number = 1 (Case column 1, Table 1)

Figure 8. Effect of heat transfer and friction on the Richardson Number of a ceiling jet. Initial Richardson Number = 2 (Case column 1, Table 1)

Figure 9. Effect of heat transfer and friction on a ceiling jet depth. Initial Richardson Number = 2 (Case column 1, Table 1).

Figure 10. Effect of heat transfer and friction on a ceiling jet flow. Initial Richardson Number = 2 (Case column 1, Table 1).

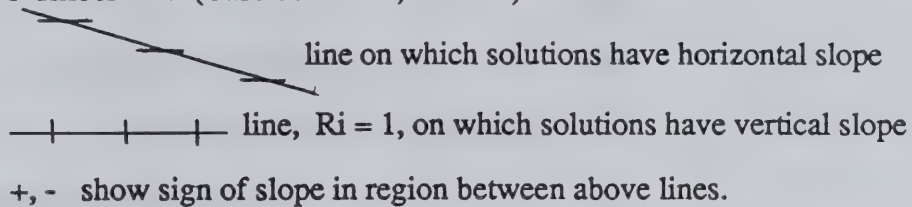


Figure 11. Richardson Number for Chobotov (16) experiment

⊙ Experimental result

———— Present theory with data column 2, Table 1 and various friction factors.

△ Present theory with node at end of experimental channel

----- Arbitrary assumption $Ri = Ri_0$ which gives "best fit" to data.

Figure 12. Ceiling jet depth for Chobotov (16) experiment

⊙ Experimental result

———— Present theory with data column 2, Table 1, and various friction factors

△ Present theory with node at end of experimental channel

X Arbitrary assumption $Ri = Ri_0$ which gives "best fit" to data

// Chobotov (16) boundary layer theory with arbitrary assumption $Ri = 1$.

Figure 13. Effect of heat transfer and friction on the ceiling jet in the Chobotov (16) experiment




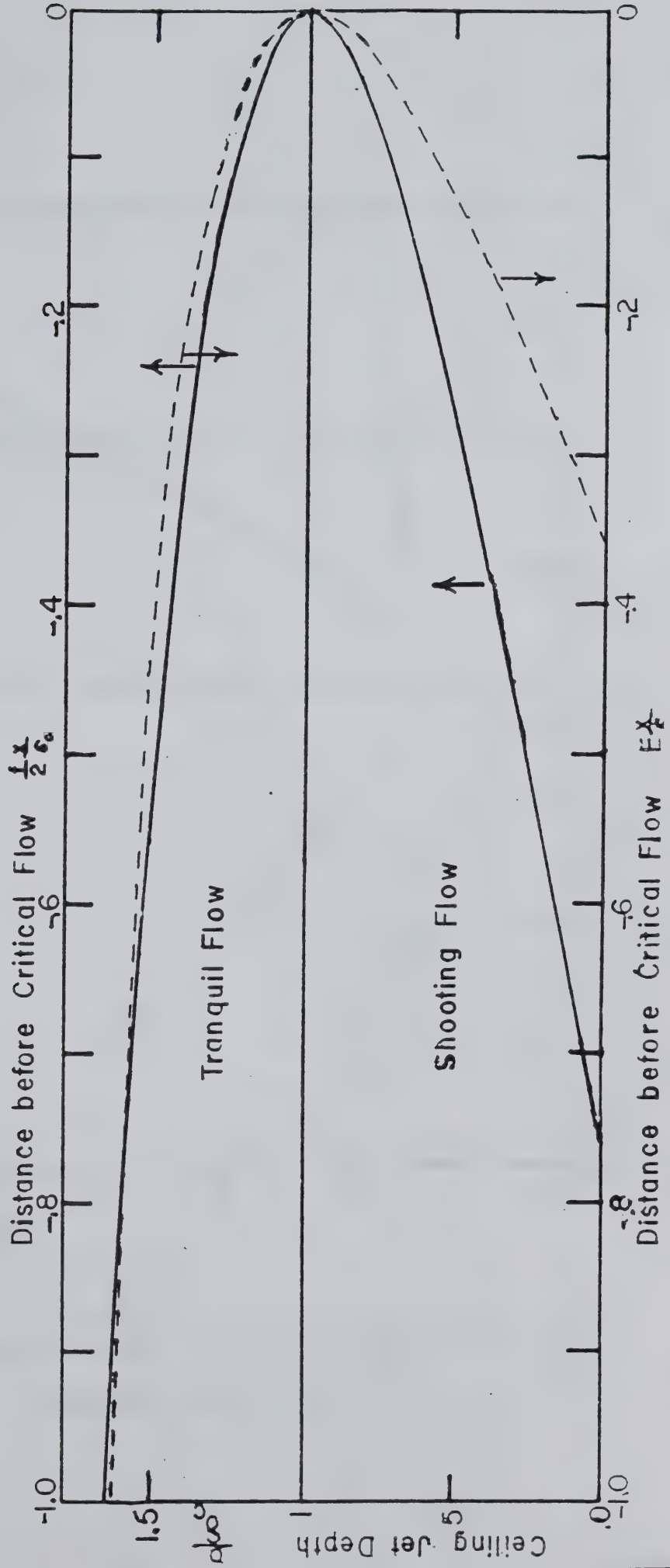
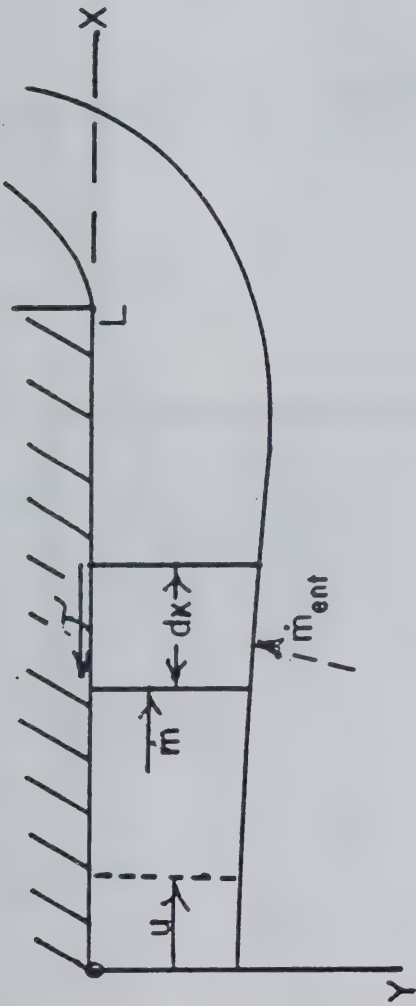
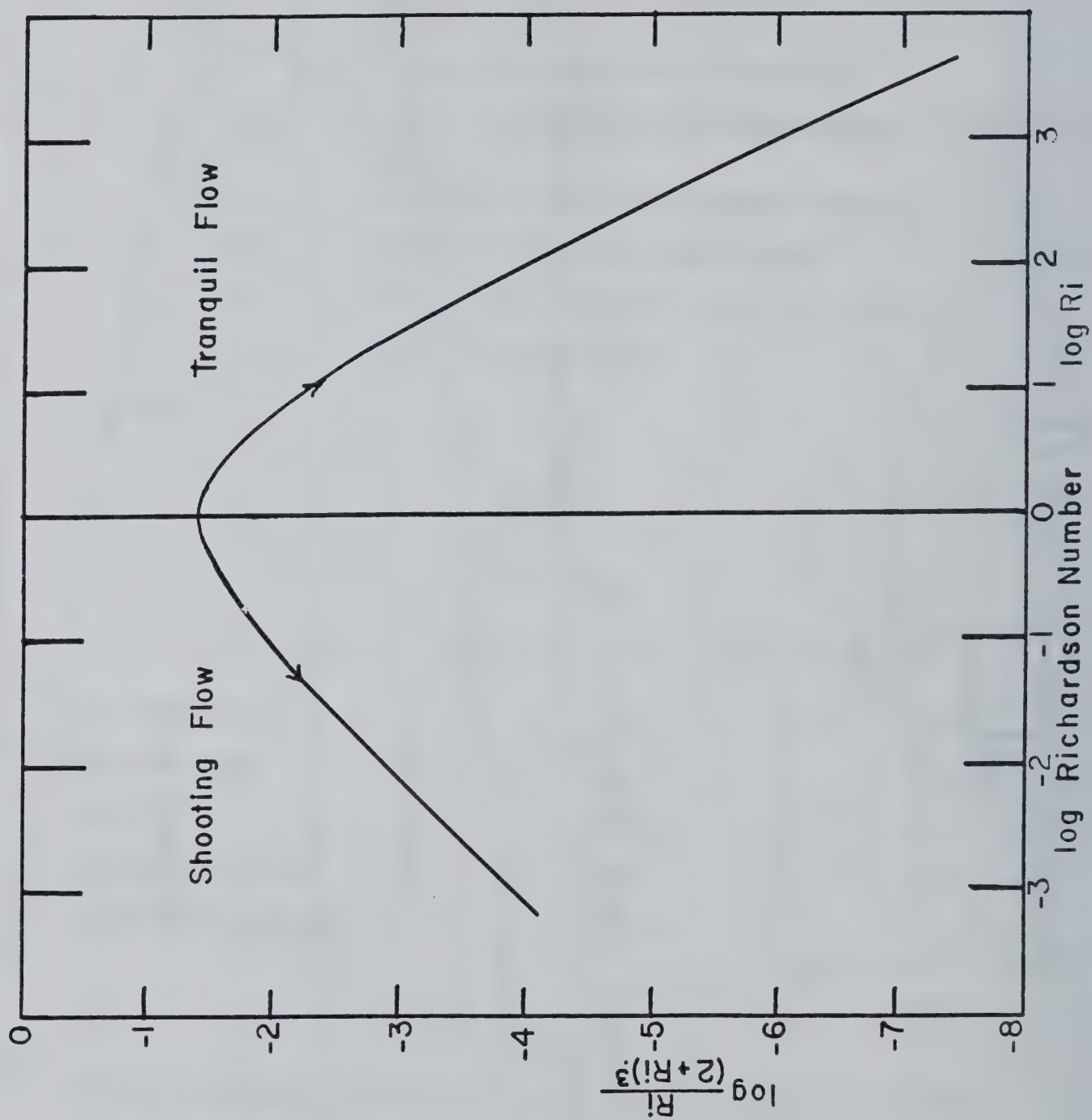
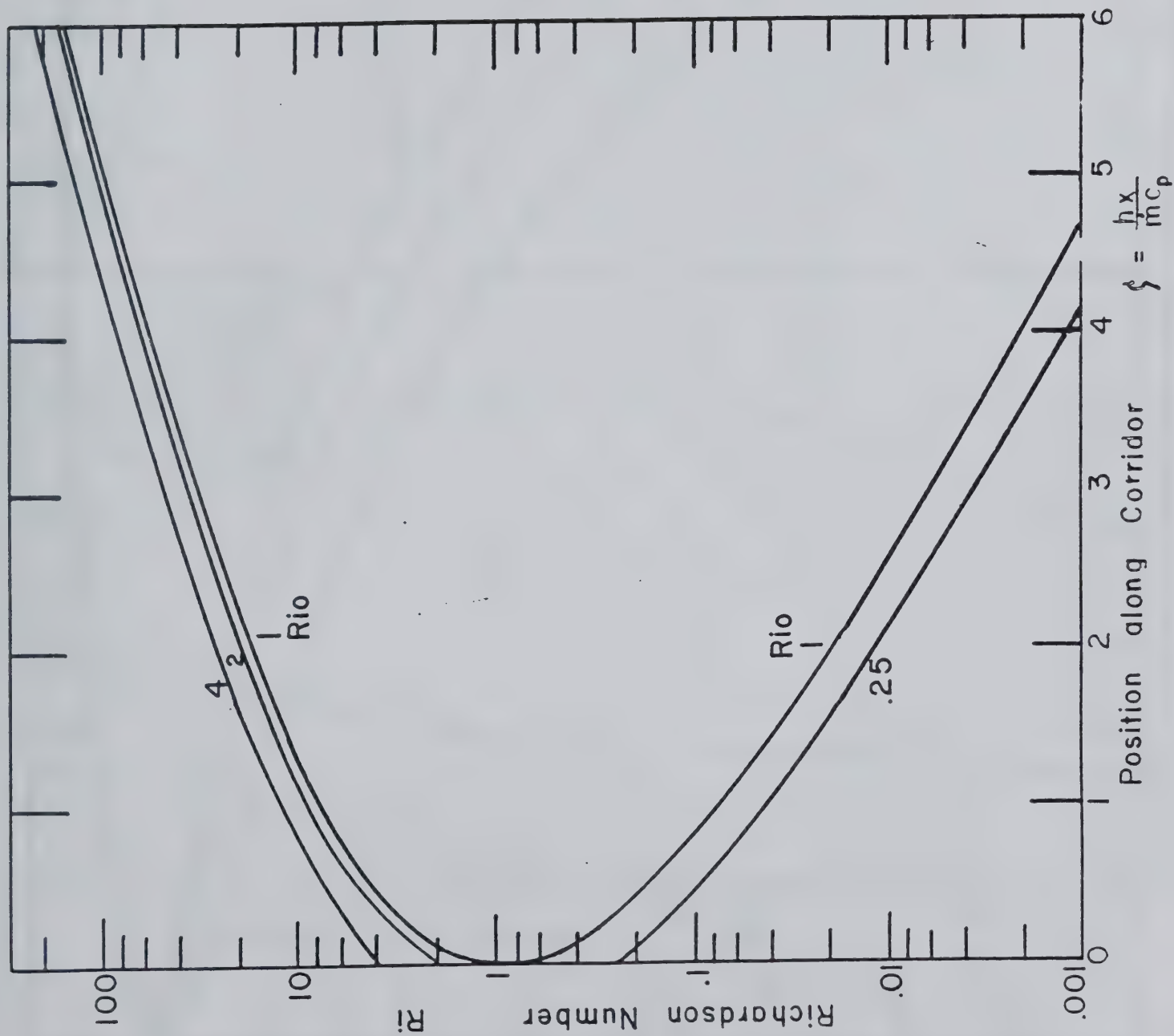
-  Present theory with data column 2, Table 1, and various friction factors
 Line on which solutions have horizontal slope
 Lines, $Ri = 1$ different f , on which solutions have vertical slope
 + , - show sign of slope in region between above lines
 N1 Node implied by experimental initial data
 N2 Node moved to the end of the experimental channel
 - - - - - Solution from node at end.

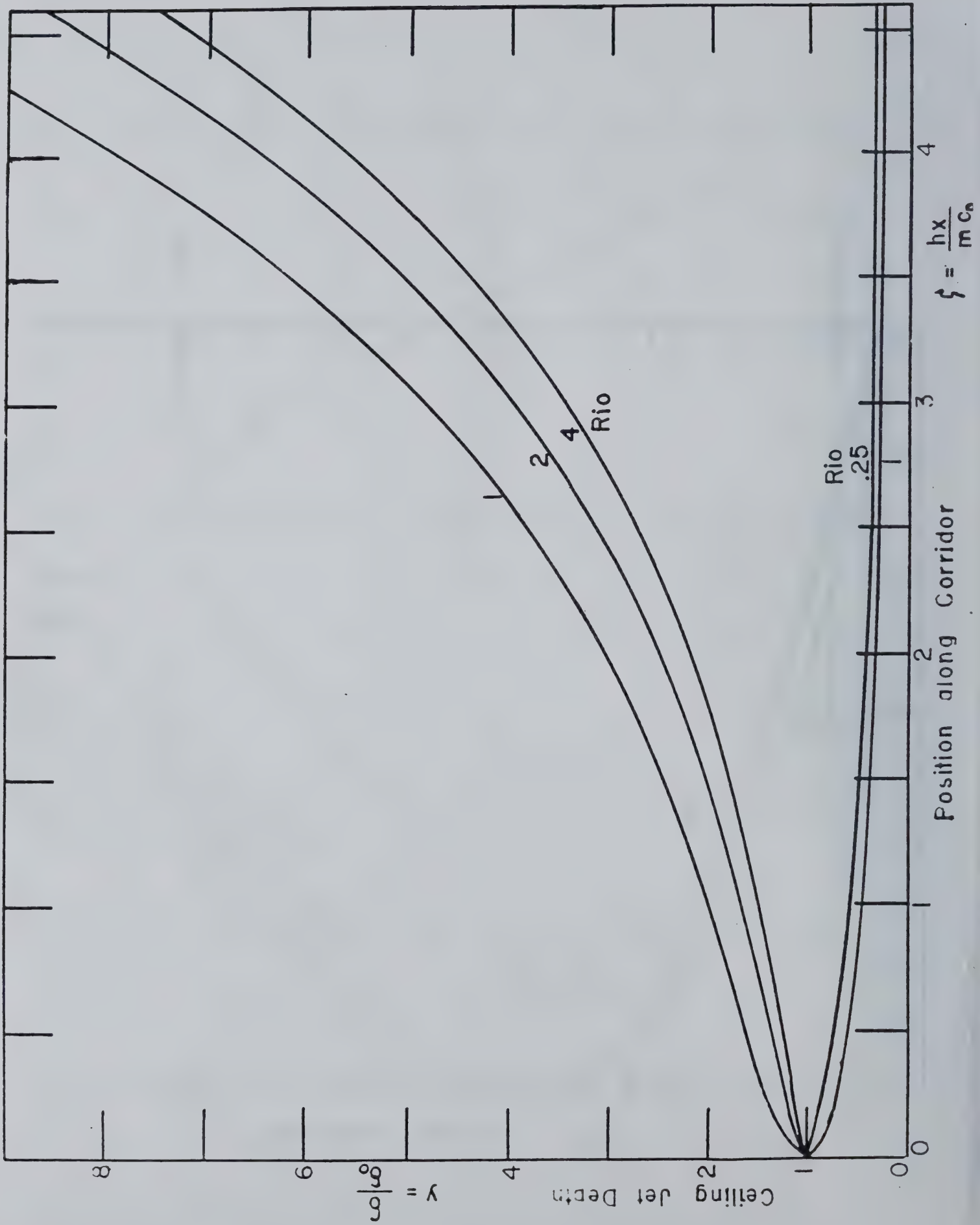
TABLE 1

	I	II
Ambient temperature	300	294
Initial temperature	800	384.3
Mass flux	.16667	.025
Heat transfer coefficient	41.65	10.6
Initial Richardson Number	various	1.195
$\frac{h}{\dot{m} c_p}$.24694	.41897
Distance along corridor x meters	4.0496 ζ	2.3868 ζ

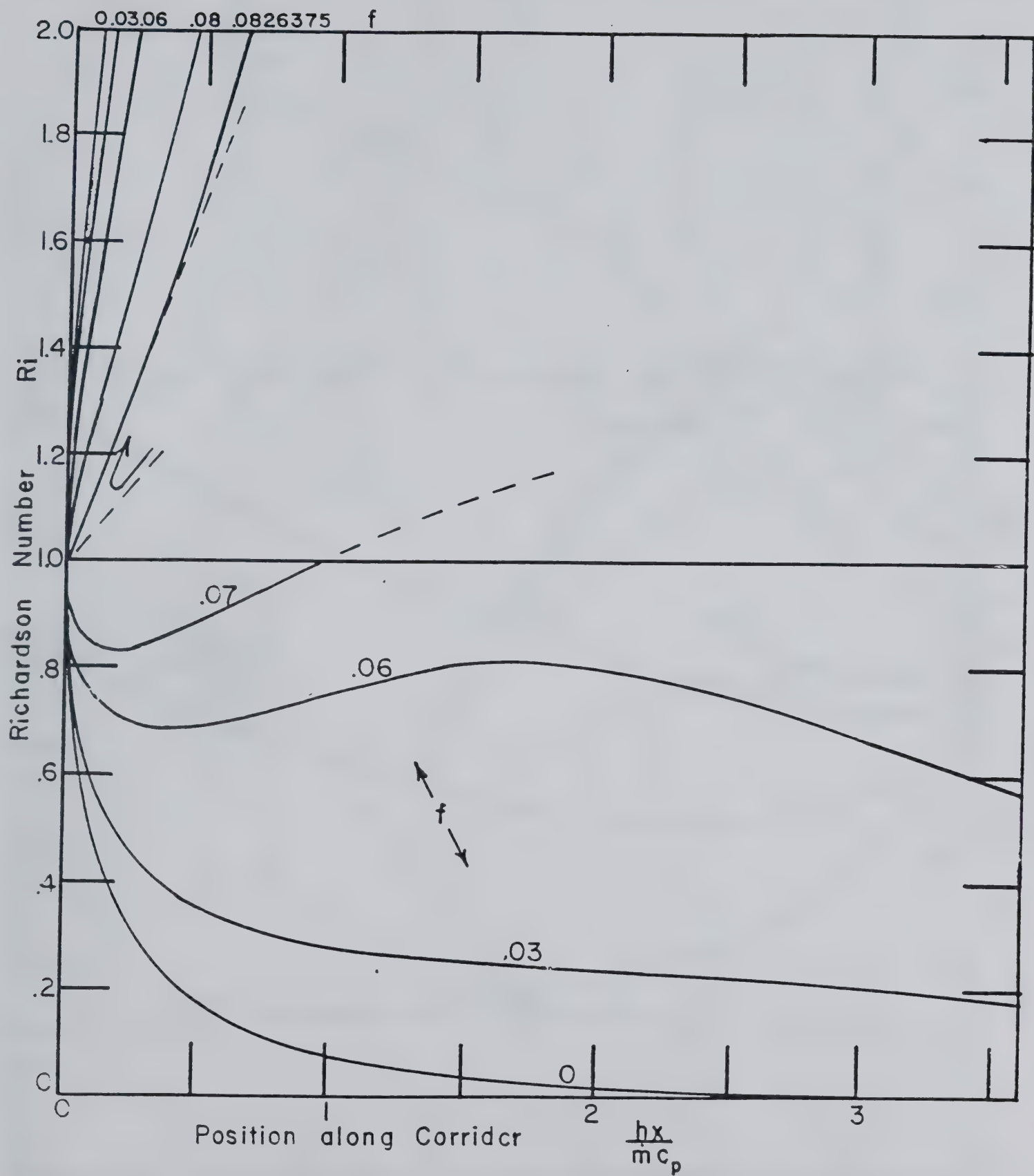


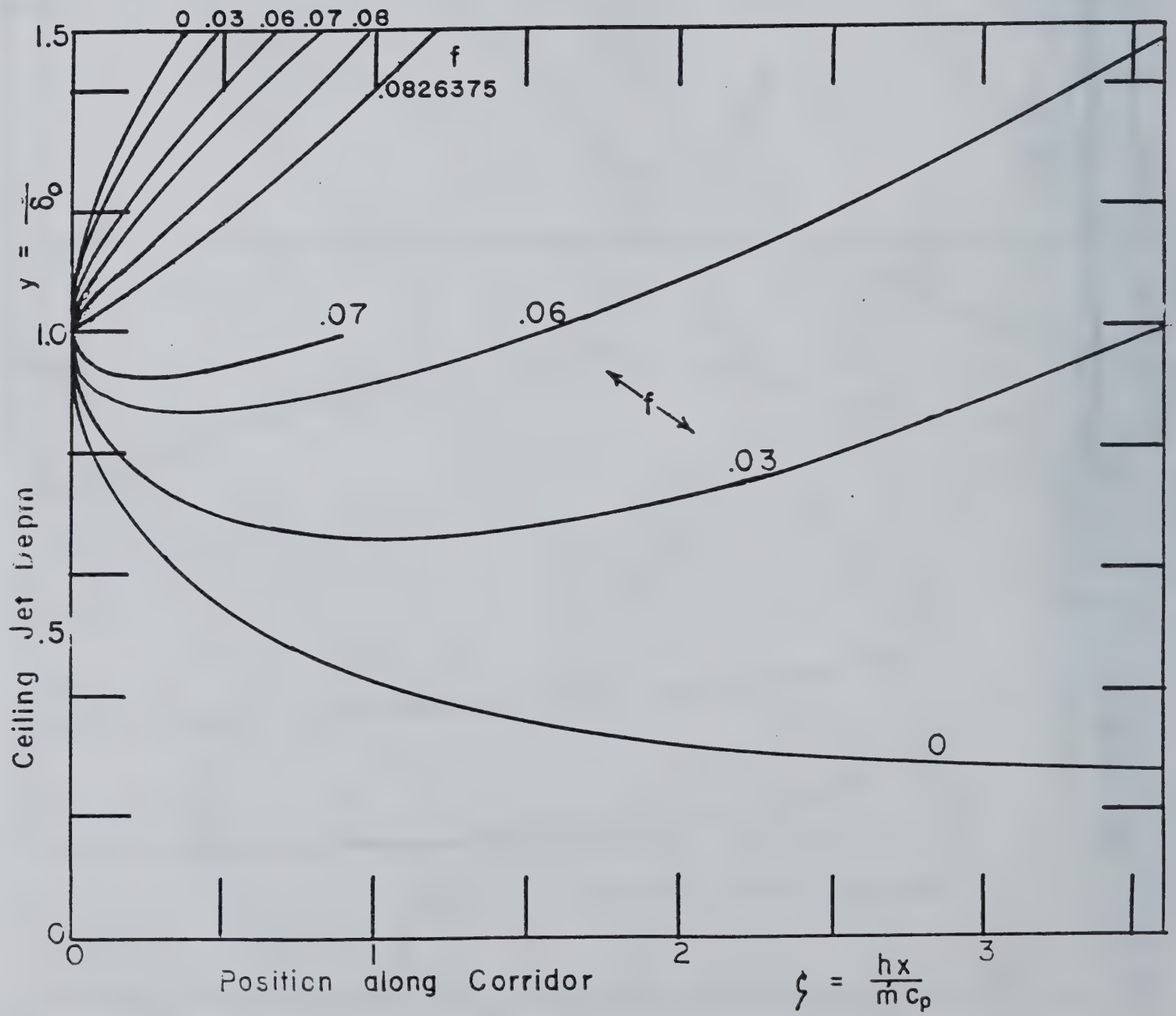


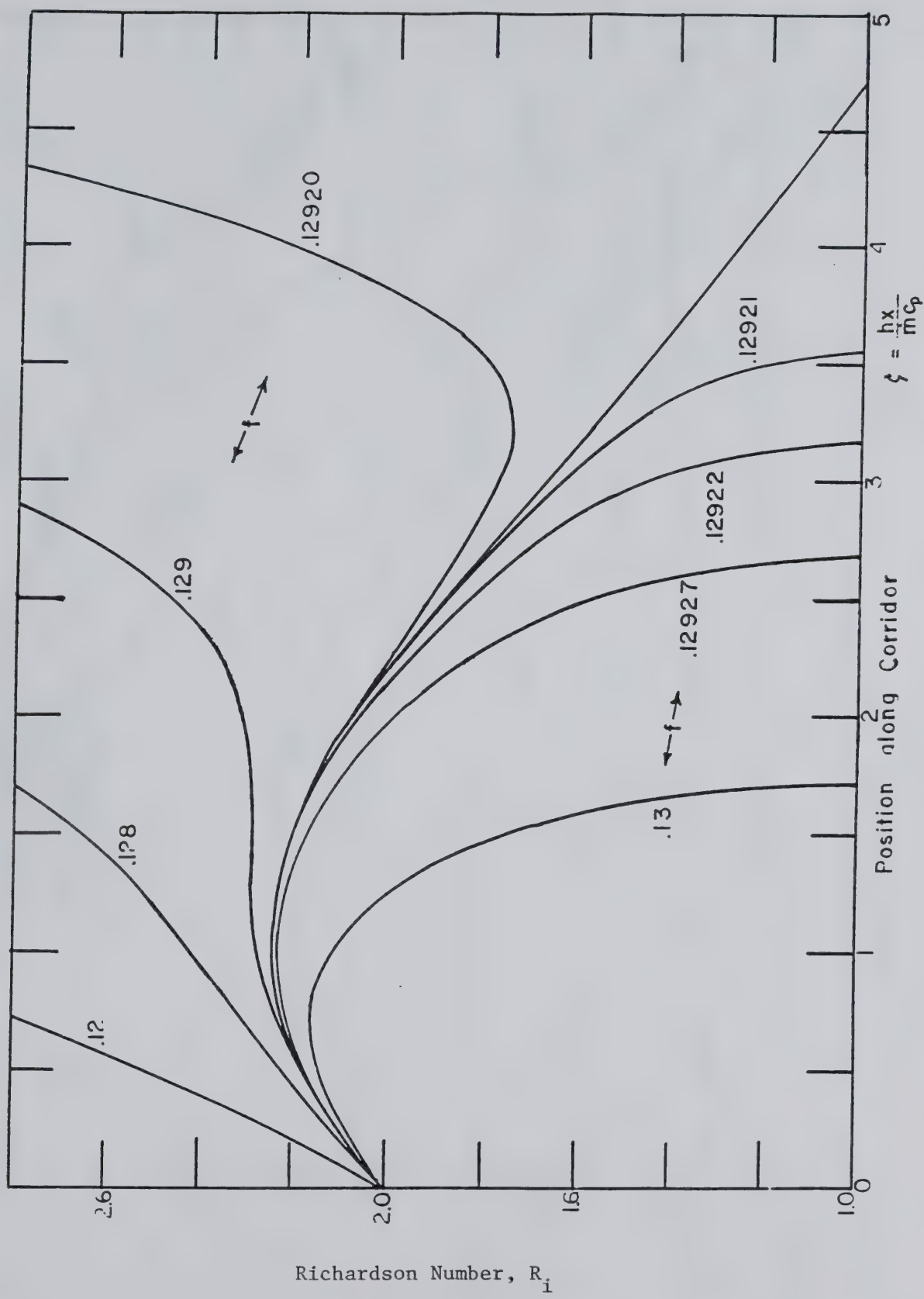


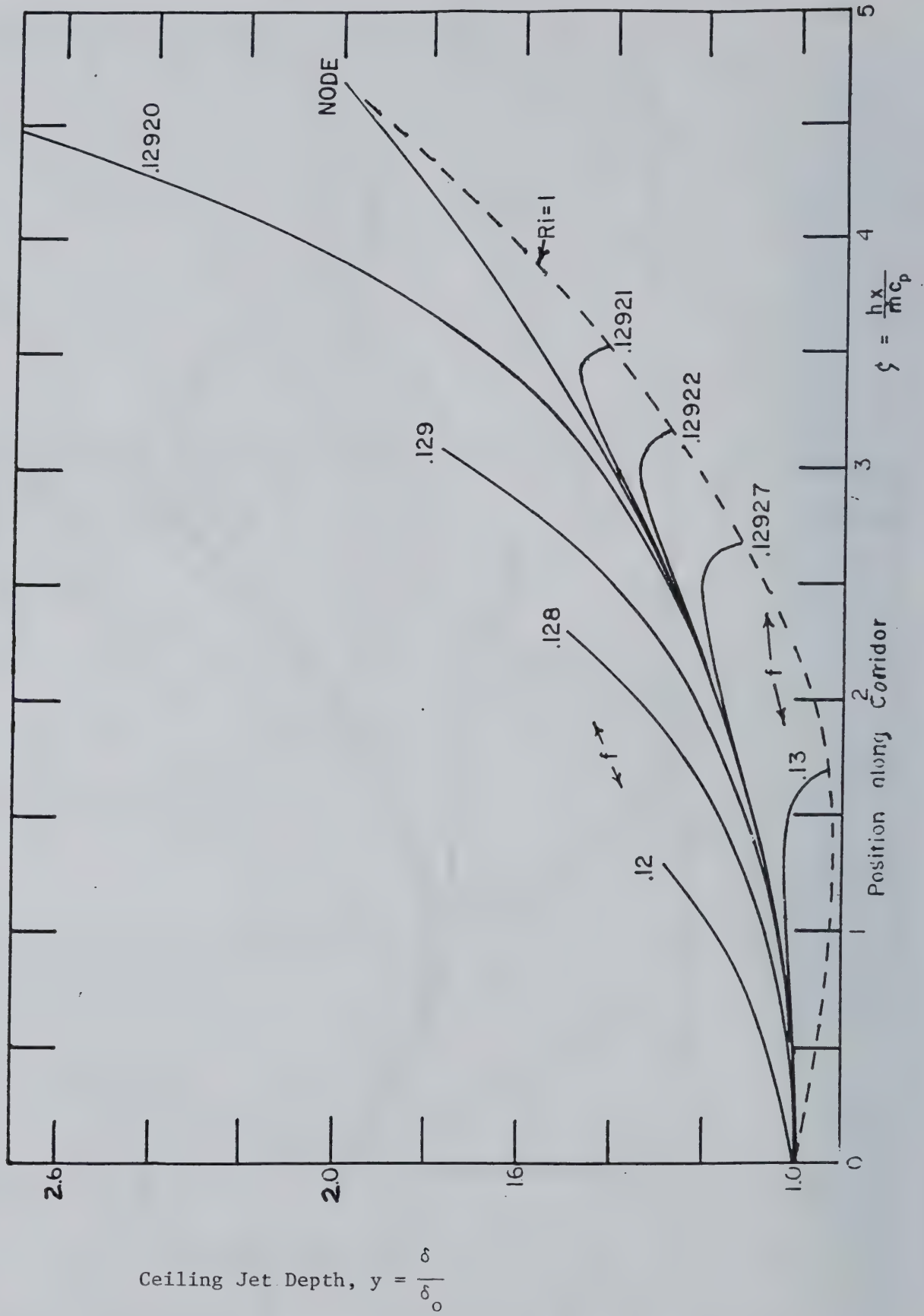


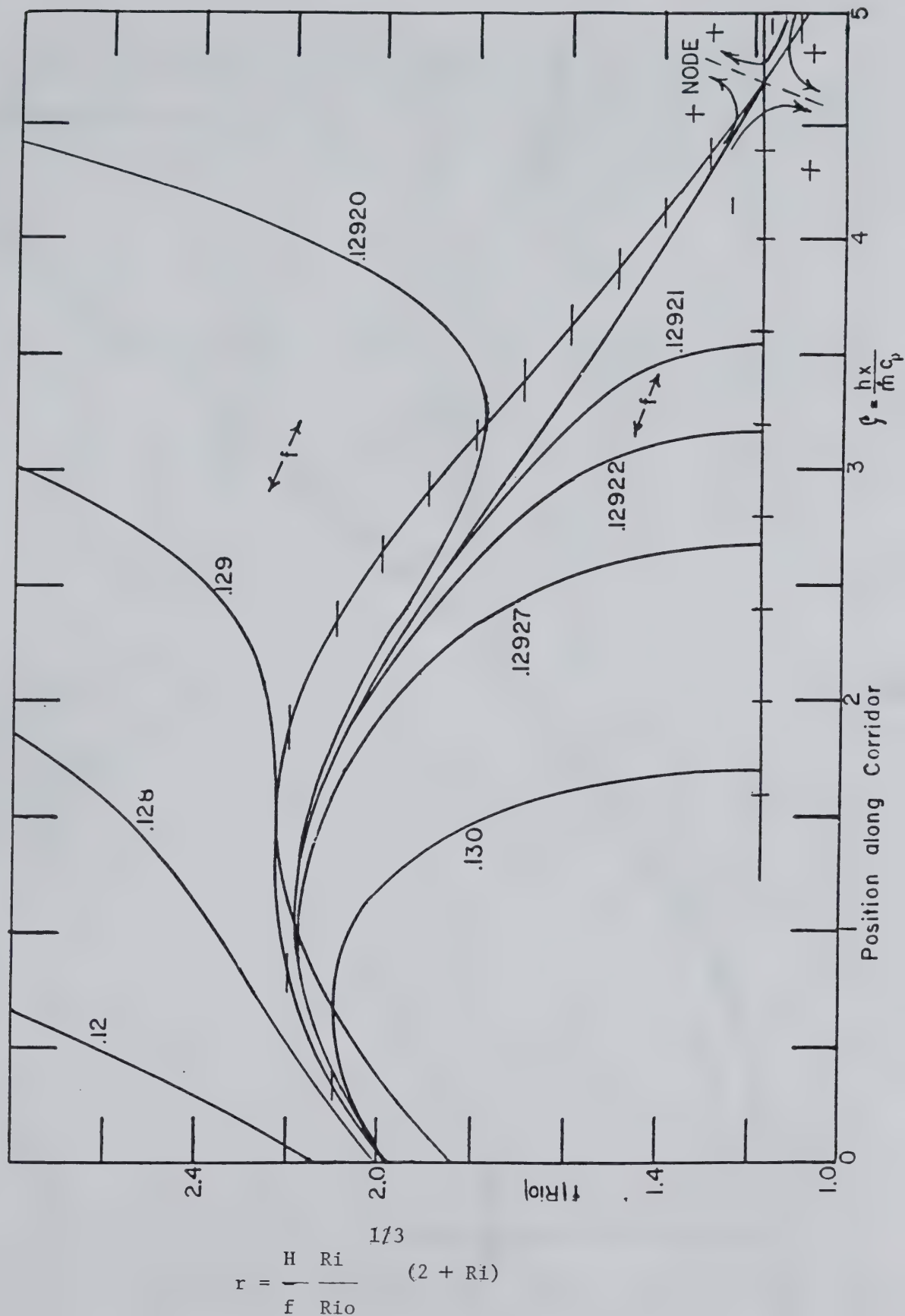
(5)

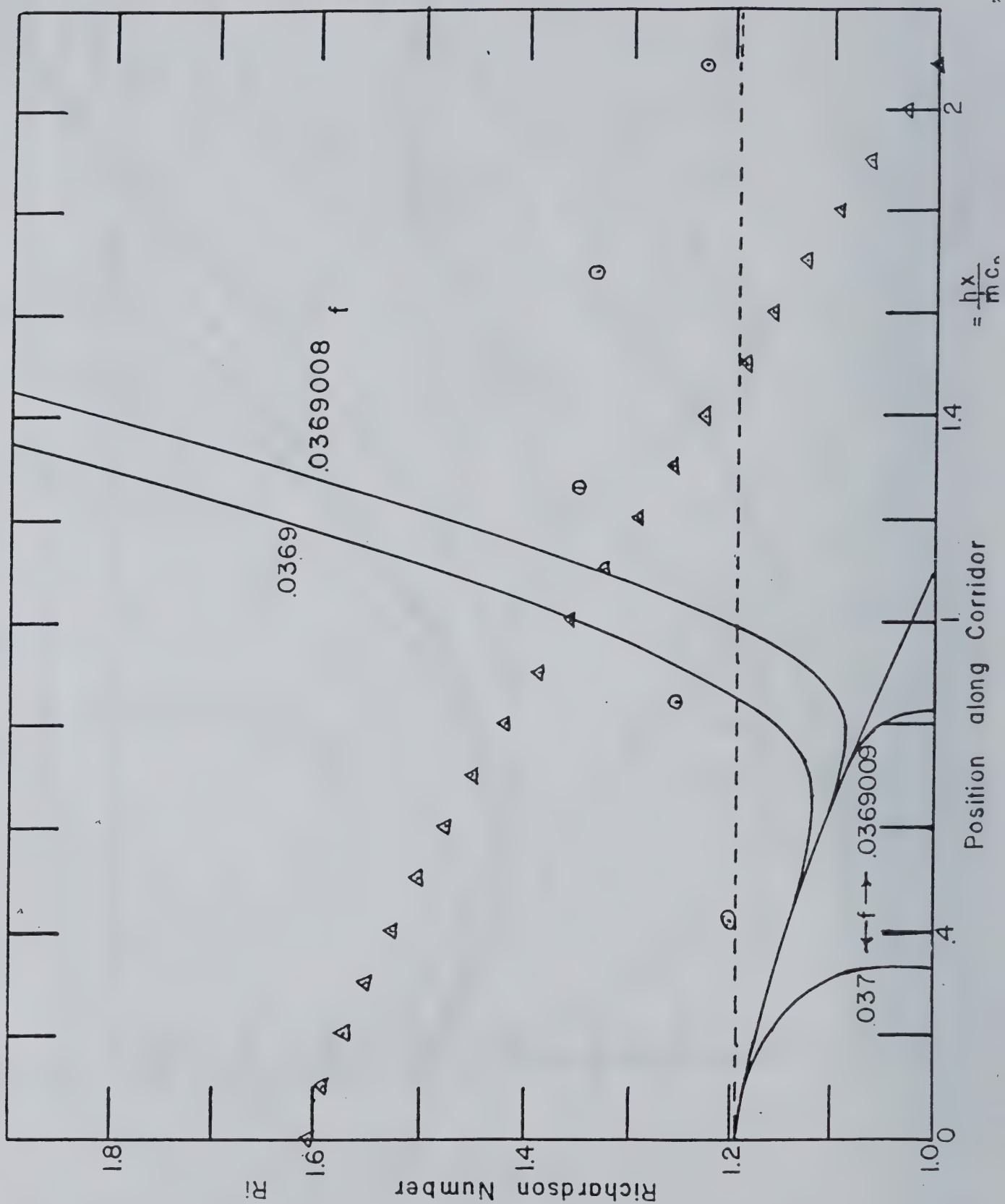


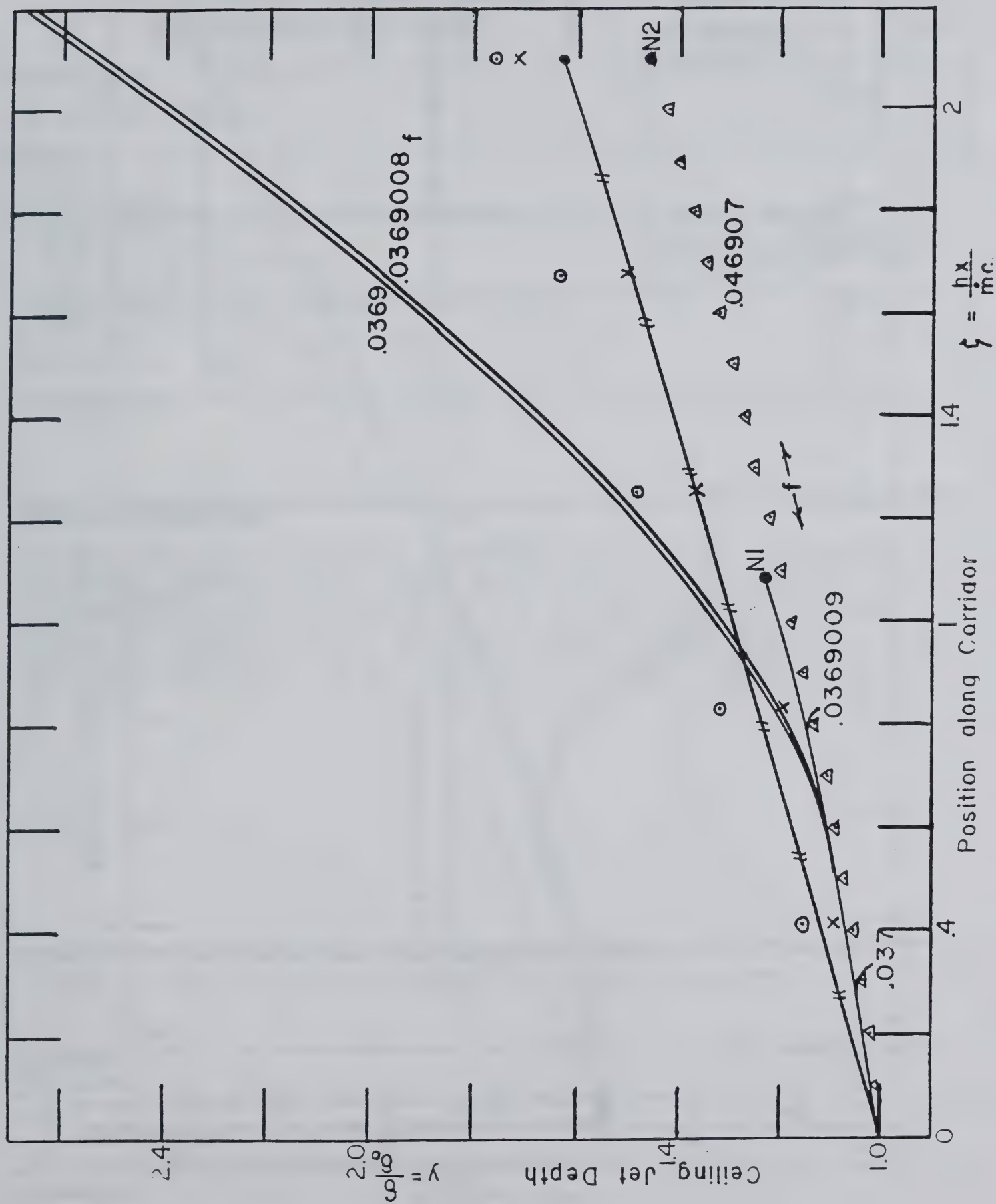


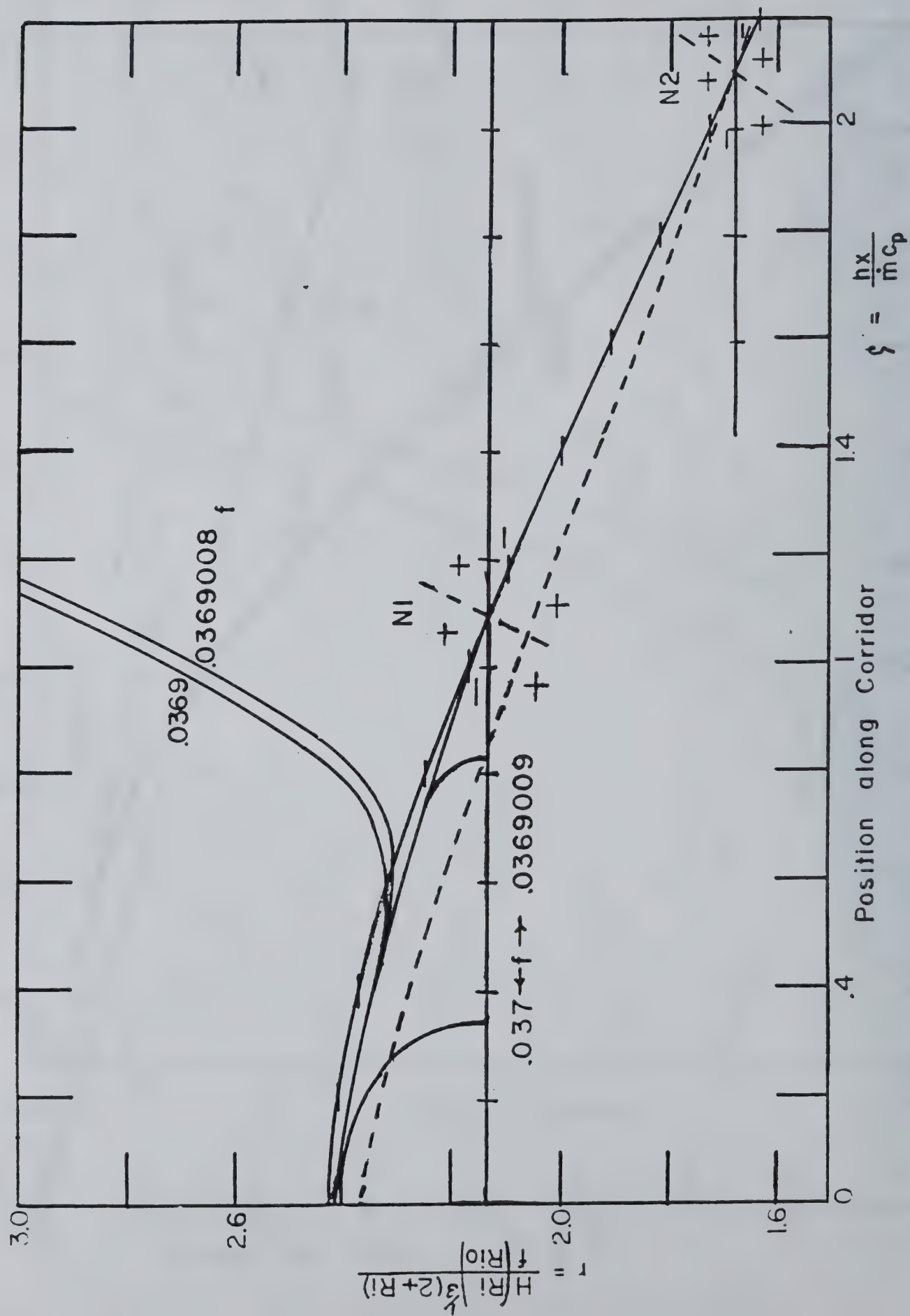












NIST-114A
(REV. 3-90)

U.S. DEPARTMENT OF COMMERCE
NATIONAL INSTITUTE OF STANDARDS AND TECHNOLOGY

BIBLIOGRAPHIC DATA SHEET

1. PUBLICATION OR REPORT NUMBER
NIST-GCR-90-582

2. PERFORMING ORGANIZATION REPORT NUMBER

3. PUBLICATION DATE
December 1990

4. TITLE AND SUBTITLE

The Ceiling Jet in Fires

5. AUTHOR(S)

Howard W. Emmons

6. PERFORMING ORGANIZATION (IF JOINT OR OTHER THAN NIST, SEE INSTRUCTIONS)

Harvard University
Division of Applied Sciences
Cambridge, MA 02138

7. CONTRACT/GRANT NUMBER

NIST Grant 60NANB8D0845

8. TYPE OF REPORT AND PERIOD COVERED

October 1990

9. SPONSORING ORGANIZATION NAME AND COMPLETE ADDRESS (STREET, CITY, STATE, ZIP)

U.S. Department of Commerce
National Institute of Standards and Technology
Gaithersburg, MD 20899

10. SUPPLEMENTARY NOTES

11. ABSTRACT (A 200-WORD OR LESS FACTUAL SUMMARY OF MOST SIGNIFICANT INFORMATION. IF DOCUMENT INCLUDES A SIGNIFICANT BIBLIOGRAPHY OR LITERATURE SURVEY, MENTION IT HERE.)

The steady ceiling jet is examined with a simplified "top hat" theory. Friction causes the jet to change downstream with flow, depth, and/or hydraulic jump adjustments to produce Richardson Number = 1 at the corridor exit, just as in hydraulics. Entrainment has a qualitative effect identical to friction, although there are quantitative differences. Heat transfer has, however, the opposite effect; the Richardson Number moves away from 1 as the flow proceeds. When all effects are included, high friction cases are predictable, while low friction cases are not. New experimental studies are needed to locate the reasons.

12. KEY WORDS (6 TO 12 ENTRIES; ALPHABETICAL ORDER; CAPITALIZE ONLY PROPER NAMES; AND SEPARATE KEY WORDS BY SEMICOLONS)

ceiling jets; corridors; hydraulic approximation; room fires; smoke movement

13. AVAILABILITY

☒ UNLIMITED
☐ FOR OFFICIAL DISTRIBUTION. DO NOT RELEASE TO NATIONAL TECHNICAL INFORMATION SERVICE (NTIS).
☐ ORDER FROM SUPERINTENDENT OF DOCUMENTS, U.S. GOVERNMENT PRINTING OFFICE, WASHINGTON, DC 20402.
☒ ORDER FROM NATIONAL TECHNICAL INFORMATION SERVICE (NTIS), SPRINGFIELD, VA 22161.

14. NUMBER OF PRINTED PAGES

5]

15. PRICE

A04

